Gain Scheduling Dual Mode MPC for a Solar Thermal Power Plant

A. Alsharkawi * **J. A. Rossiter** **

* *Department of Automatic Control and Systems Engineering, University of Sheffield, Sheffield, S1 3JD, UK (e-mail: aalsharkawi1@sheffield.ac.uk*
** *Department of Automatic Control and Systems Engineering, University of Sheffield, Sheffield, S1 3JD, UK (e-mail:j.a.rossiter@sheffield.ac.uk*

Abstract: A nonlinear gain scheduling control strategy is proposed for a concentrated solar thermal power plant. The strategy involves the identification of local linear time-invariant state space models around a family of operating points, the design of corresponding local linear dual mode model-based predictive controllers and the selection of an appropriate scheduling variable to govern the switching. The local models are estimated directly from input-output data using a subspace identification method while taking into account the frequency response of the plant. Input-output data are obtained from a nonlinear simulation model of the plant rather than the plant itself. The effectiveness of the proposed control strategy in terms of tracking and disturbance rejection is evaluated through two different scenarios created in a nonlinear simulation environment.

Keywords: Solar thermal power plant; Subspace identification; Resonant modes; Dual mode model-based predictive control; Nonlinear control; Gain scheduling.

1. INTRODUCTION

The significant global rise in the consumption of electricity and fossil fuels (coal, oil and natural gas) since the early 1970s and hence the high levels of greenhouse gas emissions and their contribution to climate change IEA (2014) are all driving factors in the desire to develop clean and sustainable energy solutions. The US National Science Foundation in 1972 stated that "Solar Energy is an essentially inexhaustible source potentially capable of meeting a significant portion of the nation's future energy needs with a minimum of adverse environmental consequences... The indications are that solar energy is the most promising of the unconventional energy sources...".

Solar energy can be converted by thermal means into electrical energy using concentrated solar power (CSP) technology Goswami et al. (2000). The application of CSP technology is expected to have a major role in long-term energy supply and thus be a key element in power security Aringhoff et al. (2005). Parabolic trough, linear Fresnel reflector, solar tower and parabolic dish are the most common types of CSP technology. These four share the same principle of operation; electricity is generated by converting solar energy into stored heat energy which in turn is used to drive a power cycle, for example a steam turbine or a heat engine Philibert (2010).

The scope of this paper will be limited to the application of parabolic trough technology. Parabolic trough stands out among the rest of the technologies as the most mature and reliable technology and indeed forms the bulk of current commercial CSP plants Philibert (2010).

The parabolic trough technology-based ACUREX plant is considered in this paper. ACUREX is one of the research facilities of the Plataforma Solar de Almera (PSA) in the province of Almeria in south-east Spain. The plant has provided opportunities for many researchers across academia and industry to explore the main dynamics of CSP technology and thus to evaluate various model forms and control strategies. A detailed description of the plant can be found in Camacho et al. (2012).

Collectors of parabolic trough technology are parabolic in shape and concentrate the incident solar radiation onto a receiver tube that is placed at its focal line. A heat transfer fluid (HTF) is heated as it flows through the receiver tube and circulates through a distributed solar collector field. The heated HTF then passes through a series of heat exchangers to produce steam which in turn is used to drive a steam turbine to generate electricity Aringhoff et al. (2005). One of the biggest challenges of the process is to maintain the field outlet temperature at a desired level despite changes, mostly in solar radiation, field inlet temperature, or ambient temperature. This can be handled efficiently by manipulating the volumetric flow rate of the HTF through advanced control strategies Camacho et al. (2012). A comprehensive survey of the modelling and control approaches for distributed solar collectors fields is presented in Camacho et al. (2007a,b).

In a previous work Alsharkawi and Rossiter (2016), it was argued that the plant ACUREX possesses resonance characteristics, namely resonant modes and for a linear control system design, high order linear models are required to capture these dynamic characteristics and hence attain a high control performance. There is a need to overcome some of the drawbacks of the gain scheduling (GS) control strategies reported in Camacho et al. (1997); Johansen et al. (2000), where the plant resonant modes had been considered explicitly through the identification of high order linear models around a family of operating points. The drawbacks can be summarized as follows:

- Poor Pseudo-Random Binary Sequence (PRBS) design in Johansen et al. (2000), where the prior knowledge of the plant was not taken into account. The design of the frequency band and amplitude of the PRBS signal is not reported in Camacho et al. (1997).
- Local high order linear models were estimated from experimental data of the plant and hence an optimal model accuracy will never be achieved due to the slow dynamics of the plant and the fast changes in the operating conditions (e.g. solar radiation) within a limited time frame.
- Decomposition of the normal region of operation of the plant is selected in Johansen et al. (2000) such that the gain and time constant of the local models differ by less than a factor of 2 between any neighbouring regions. This relies on the big assumption that the local models are exactly correct at the centre points of their corresponding regions.
- Plant safety constraints were ignored in the control system design in Johansen et al. (2000) and poorly investigated in Camacho et al. (1997) when the field outlet temperature was restricted to not exceed a desired reference under any circumstances.

The first few steps towards an improved GS control strategy were carried out in Alsharkawi and Rossiter (2016), when a linear time-invariant (LTI) state space model was estimated directly from input-output data around a nominal operating point through a subspace identification method and a corresponding local dual mode model-based predictive control (MPC) strategy was designed for tracking and disturbance rejection. This paper aims to continue the work started in Alsharkawi and Rossiter (2016) by estimating LTI state space models around a family of operating points and designing corresponding dual mode MPC controllers within a GS framework. The region of operation is decomposed in a more sophisticated manner through a best fit criterion and plant safety constraints are incorporated systematically and handled online over a wide range of operation.

This paper is organised as follows: mathematical models of the plant are described in section 2; section 3 is devoted to the phenomena of resonant modes and system identification; section 4 outlines the local dual mode MPC design and discusses the nonlinear GS control strategy. Section 5 presents the simulation results for two commonplace scenarios and the main findings and some concluding remarks are presented in section 6.

2. MATHEMATICAL MODELS

This section gives a brief description of two mathematical models of the ACUREX plant: a nonlinear distributed parameter model for simulation purposes followed by a nonlinear lumped parameter model for control design purposes.

2.1 Nonlinear Distributed Parameter Model

The distributed solar collector field of the ACUREX plant consists of 480 single axis parabolic trough collectors which are arranged in 10 parallel loops each of length 172 m. The dynamic behaviour of the plant can be described by the following set of energy balance partial differential equations (PDEs):

$$\begin{aligned} &\rho_m C_m A_m \frac{\partial T_m}{\partial t} = n_o G I - D_o \pi H_l (T_m - T_a) \\ &- D_i \pi H_t (T_m - T_f) \\ &\rho_f C_f A_f \frac{\partial T_f}{\partial t} + \rho_f C_f q \frac{\partial T_f}{\partial x} \\ &= D_i \pi H_t (T_m - T_f) \end{aligned} \tag{1}$$

where the subindex m refers to the metal of the receiver tube and f to the HTF Camacho et al. (2012). Table 1 gives a description of all the variables and parameters and lists their SI units.

Table 1. Variables and parameters.

Symbol	Description	SI unit
ρ	Density	kg/m^3
C	Specific heat capacity	$J/kg°$C
A	Cross-sectional area	m^2
T	Temperature	°C
t	Time	s
I	Solar radiation	W/m^2
n_o	Mirror optical efficiency	−
G	Mirror optical aperture	m
D_o	Outer diameter of the receiver tube	m
H_l	Global coefficient of thermal losses	$W/m°$C
T_a	Ambient temperature	°C
D_i	Inner diameter of the receiver tube	m
H_t	Coefficient of metal-fluid heat transfer	$W/m^2°$C
q	HTF volumetric flow rate	m^3/s
x	Space	m

A nonlinear simulation model of the plant can be constructed by dividing the receiver tube into n $(n = 1, 2, ...)$ segments each of length Δx, and hence the nonlinear distributed parameter model in (1) can be approximated by the following set of ordinary differential equations (ODEs):

$$\begin{aligned} &\rho_m C_m A_m \frac{dT_{m,n}}{dt} = n_o G I - D_o \pi H_l (T_{m,n} - T_a) \\ &- D_i \pi H_t (T_{m,n} - T_{f,n}) \\ &\rho_f C_f A_f \frac{dT_{f,n}}{dt} + \rho_f C_f q \frac{T_{f,n} - T_{f,n-1}}{\Delta x} \\ &= D_i \pi H_t (T_{m,n} - T_{f,n}) \end{aligned} \tag{2}$$

with the boundary condition $T_{f,0} = T_{f,inlet}$ (field inlet temperature) and H_l,H_t,ρ_f and C_f being time−varying.

It has been found in Alsharkawi and Rossiter (2016) that dividing the receiver tube into 7 segments is a reasonable trade-off between the prediction accuracy and computational burden while still adequate enough to capture the resonant modes of the plant. The nonlinear lumped parameter submodels in (2) are implemented and solved efficiently using the MATLAB solver ODE45 (an explicit Runge-Kutta method) where the temperate distribution in the receiver tube and HTF can be easily accessed at any point in time and for any segment n.

2.2 Nonlinear Lumped Parameter Model

The dynamic behaviour of the ACUREX plant can also be described by a simple nonlinear lumped parameter model. Variation in the internal energy of the fluid can be described by:

$$C\frac{dT_f}{dt} = n_o SI - QP_{cp}(T_f - T_{f,inlet}) - H_l(T_{mean} - T_a) \quad (3)$$

where S is the collectors solar field effective surface, Q is the HTF volumetric flow rate, P_{cp} is a factor that takes into account some geometrical and thermal properties and T_{mean} is the mean of T_f and $T_{f,inlet}$ Camacho et al. (2012).

3. RESONANT MODES AND SYSTEM IDENTIFICATION

The resonance phenomena of the ACUREX plant are described in Meaburn and Hughes (1993) as resonant modes that lie well within the desired control bandwidth. The phenomena arise due to the relatively slow flow rate of the HTF and the length of the receiver tube involved. It has also been found that the phenomena have a significant impact on the control performance and hence modelling the resonant modes sufficiently is crucial to ensure high control performance with adequate robustness.

One of the first steps towards an effective modelling of the resonant modes is a proper choice and design of excitation signals. Here PRBS-type excitation signals were chosen. A PRBS is a deterministic binary signal with white noise like properties and ideally suited for linear identification. However, the white noise like properties are only valid for full-length PRBS signals with a clock period approximately equals the process sampling time Zhu (2001).

Since the dynamics of the ACUREX plant are mainly characterised by the flow rate of the HTF (Camacho et al., 2012), the nonlinear simulation model of the plant described by the system in (2) was excited with a set of full-length PRBS signals with an amplitude of 0.0005 m^3/s and a clock period equal to the process sampling time 39 s (the process time constant is around 6 min) around the operating points 0.004, 0.006, 0.008 and 0.010 m^3/s. The identification process assumed steady state operating conditions ($I_{nom} = 674.75\ W/m^2$, $T_{f,inlet,nom} = 183$ °C and $T_{a,nom} = 28$ °C) and used a data set of 1100 samples for each of the nominal operating points.

Compact local LTI state space models were identified around the nominal operating points using a subspace identification method (N4SID). Subspace identification methods are computationally efficient and overcome some of the major problems encountered in classical identification methods, i.e, parametrization, convergence and model reduction Van Overschee and De Moor (1996). The general form of a discrete-time LTI state space model is given as:

$$\begin{aligned} x_{k+1} &= Ax_k + Bu_k + \xi_k \\ y_k &= Cx_k + Du_k + \eta_k \end{aligned} \quad (4)$$

where $x_k \in \Re^{n\times1}$, $u_k \in \Re^{m\times1}$, $y_k \in \Re^{l\times1}$, $\xi_k \in \Re^{n\times1}$ and $\eta_k \in \Re^{l\times1}$ are the state vector, input vector, output vector, process noise and measurement noise respectively at discrete time instant k. A, B, C and D are the coefficient matrices of appropriate dimensions.

The local models were estimated under the assumptions that there is no direct feedthrough from the input to the output ($D = 0$) and the system is deterministic ($\xi_k = \eta_k = 0$). Initial states were set to zero during the estimation process and the weighting scheme canonical variable algorithm (CVA) was used for the singular value decomposition (SVD). The N4SID method and the associated weighting scheme CVA are discussed in Van Overschee and De Moor (1996) and Larimore (1990) respectively.

Model order was estimated for each of the local models by inspecting the singular values of a certain covariance matrix constructed from the observed data. Model order and best fit criterion are shown in Table 2. Local models 1, 2, 3, and 4 refer to the nominal operating points around 0.004, 0.006, 0.008 and 0.010 m^3/s respectively.

Table 2. Model order and best fit criterion

Local model	Model order	Best fit criterion (%)
1	4^{th}	95.07
2	4^{th}	97.16
3	4^{th}	98.05
4	5^{th}	98.51

Since the estimated local LTI state space models are mainly used for prediction within the dual mode MPC control design, the simulated model output (infinite-step ahead prediction) is validated through a best fit criterion. The criterion is given in Ljung (1995) as:

$$Bestfit = \left(1 - \frac{\sum_{i=1}^{n} |y_i - \hat{y}_i|}{\sum_{i=1}^{n} |y_i - \bar{y}|}\right) \times 100 \quad (5)$$

where y, $\hat{y}$ and $\bar{y}$ are the measured output, the simulated model output and the mean of the measured output respectively.

The best fit criterion in (5) reflects the ability of the estimated local models to reproduce the main dynamics of the plant at a given operating point and time horizon. From Table 2, one can observe that the prediction accuracy is improved as the flow rate of the HTF is increased from 0.004 to 0.010 m^3/s. This can be explained by the high nonlinearities of the plant at low flow rates (long residence time of the HTF in the collectors solar field), which has been also noticed in Stirrup et al. (2001) when a fuzzy proportional-integral (PI) controller with feedforward term was developed for the highly nonlinear part of the plant whereas a GS control strategy was developed for the more linear part.

The estimated local models capture the phenomena of resonant modes adequately as validated by inspecting the Bode plots shown in Fig. 1. One can clearly identify the resonant modes of the plant and observe the dependence of their frequencies on the flow rate of the HTF. Another observation is the changes in the steady state gain as the flow rate is increased from 0.004 to 0.010 m^3/s.

In summary it should be emphasised that the estimated local state space models are less complex than the local ARX models presented in Camacho et al. (1997); Johansen et al. (2000) in terms of model order. However, for a fair comparison, local ARX models similar to the ones used in Camacho et al. (1997); Johansen et al. (2000) were estimated using the same sets of data that had been used earlier to produce Table 2. Model order was estimated for each of the local models through Akaike's information

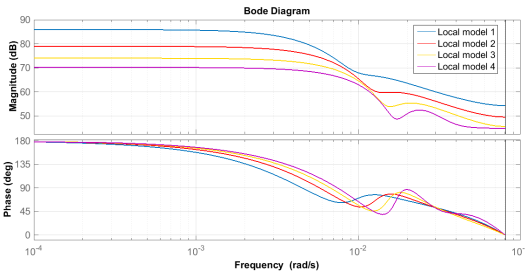

Fig. 1. Bode plots of the estimated local LTI state space models.

criterion (AIC). The order of the local ARX models in Table 3 is significantly higher than the order of the local state space models in Table 2 without having a serious impact on the prediction accuracy.

Table 3. Model order and best fit criterion

Local model	Model order	Best fit criterion (%)
1	7^{th}	94.88
2	11^{th}	97.16
3	12^{th}	98.07
4	12^{th}	98.52

4. CONTROL DESIGN

This section outlines the local dual mode MPC design and the nonlinear GS control strategy.

4.1 Dual Mode MPC

The term dual mode refers to a separation in the model predictions into transient (mode 1) and asymptotic (mode 2) predictions. The separation gives a handle on the predictions over an infinite horizon, where a simple linear feedback law can be implemented, thus allowing a reduction in the number of degrees of freedom (d.o.f) and constraints Rossiter (2003). For a deterministic version of the system in (4) and assuming no direct feedthrough, the deviation from the estimated steady state values x_{ss}, u_{ss} and y_{ss} can be expressed as:

$$\begin{aligned} \hat{x}_{k+1} &= A\hat{x}_k + B\hat{u}_k \\ \hat{y}_k &= C\hat{x}_k \end{aligned} \tag{6}$$

A standard dual mode cost function (online performance measure) J is given as:

$$J = \sum_{i=0}^{n_c-1} [\hat{x}^T_{k+1+i}\delta\hat{x}_{k+1+i} + \hat{u}^T_{k+i}\lambda\hat{u}_{k+i}] + \hat{x}^T_{k+n_c}P\hat{x}_{k+n_c} \tag{7}$$

where n_c is the number of free d.o.f., δ and λ are weighting matrices of appropriate dimensions and P is obtained from a Lyapunov equation of appropriate dimension. The cost function in (7) can be simplified to take the form of a standard quadratic programming problem with constraints and solved online as:

$$\min_{\underset{\rightarrow}{\hat{u}}} \underset{\rightarrow k-1}{\hat{u}^T} S \underset{\rightarrow k-1}{\hat{u}} + \underset{\rightarrow k-1}{\hat{u}^T} L\hat{x}_k \quad s.t. \quad M\underset{\rightarrow}{\hat{u}} \leq \gamma \tag{8}$$

where $\underset{\rightarrow k-1}{\hat{u}} = [\hat{u}_k \quad \hat{u}_{k+1} \quad \ldots \quad \hat{u}_{k+n_c-1}]^T$, S and L depend upon the matrices A, B, δ, λ and P, M is time-invariant and γ depends upon the system past input-output information. Detailed treatment of the dual mode MPC and proper definitions of the various parameters can be found in Rossiter (2003).

4.2 Nonlinear GS Control

GS is one of the most accepted nonlinear control design approaches which has found applications in many fields ranging from aerospace to process control Leith and Leithead (2000). GS control is usually seen as a way of thinking rather than a fixed design process and well-known for applying powerful linear design tools to challenging nonlinear problems Rugh and Shamma (2000). Moreover, implementation of MPC within a GS framework overcomes the major computational drawbacks of using nonlinear MPC which arise due to the non-convexity of the associated nonlinear optimization problem Chisci et al. (2003).

The design workflow of the proposed nonlinear GS control strategy involves the designing and tuning of a nominal linear dual mode MPC controller around medium operating conditions (0.006 m^3/s) and using simulations to determine the operating conditions at which the nominal controller losses robustness. Local LTI state space models around the new operating conditions were estimated and corresponding local linear dual mode MPC controllers were designed.

Having a scheduling variable to switch among the local linear dual mode MPC controllers as the plant dynamics change with time or operating conditions is an intrinsic part of the GS control strategy. Since the plant dynamics are mainly characterised by the flow rate of the HTF, Q (HTF volumetric flow rate) is used as the scheduling variable and obtained from the nonlinear lumped parameter model in (3).

Assuming steady state condition ($\frac{dT_f}{dt} = 0$) and best case scenario ($T_f = T_{f,ref}$ and $H_l = 0$), where $T_{f,ref}$ is the desired reference temperature, the model in (3) can be given as:

$$0 = n_o SI - QP_{cp}(T_{f,ref} - T_{f,inlet}) \tag{9}$$

which can be rewritten as:

$$Q = \frac{n_o SI}{P_{cp}(T_{f,ref} - T_{f,inlet})} \tag{10}$$

The relationship in (10) means that the scheduling variable Q is proportional to the solar radiation I and inversely proportional to the desired temperature change ($T_{f,ref} - T_{f,inlet}$). Schematic diagram of the proposed GS control strategy is depicted in Fig. 2.

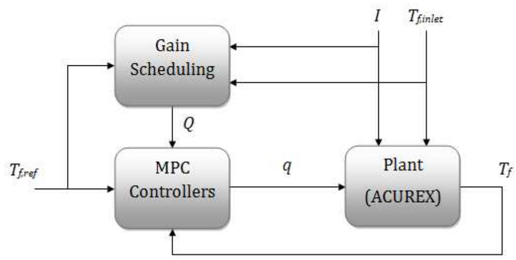

Fig. 2. GS control strategy.

Once the scheduling variable is obtained and the distinct nominal operating points are identified, the final step of the design process is to have a fine decomposition of the region of operation. In other words, the scheduling thresholds between the neighbouring local operating regions should be carefully selected so that optimal control performance is achieved. An appropriate local operating regions were identified after performing an extensive simulations, where the ability of each and every one of the local models of representing a potential thresholds was investigated through the best fit criterion in (5). Potential thresholds were identified following the same identification process discussed earlier in section 3. Scheduling thresholds $0.00475 - \alpha$, $0.00675 + \alpha$ and $0.00875 + \alpha$ m^3/s were found, where α is an uncertainty factor of less than 0.00025 m^3/s. The decomposition that has been selected can be described by the following set of if-then rules:

$$
\begin{aligned}
&if\ Q < 0.00475,\ then\\
&s = 1\\
&if\ 0.00475 \leq Q \geq 0.00675,\ then\\
&s = 2\\
&if\ 0.00675 < Q \leq 0.00875,\ then\\
&s = 3\\
&if\ Q > 0.00875,\ then\\
&s = 4
\end{aligned}
$$

where the variable s is a switch that specifies when to switch from on local model to another and accordingly from one local controller to another.

5. SIMULATION RESULTS

The effectiveness of the proposed nonlinear GS control strategy is evaluated through two different simulation scenarios. The first scenario assumes a clear day with a mean solar radiation value of 674.75 W/m^2. This scenario intends to evaluate the control performance of the proposed control strategy in terms of tracking and the associated control action. For a meaningful evaluation and interpretation of the control strategy, the control performance is compared to that with a single local dual mode MPC controller. The second scenario on the other hand intends to evaluate the robustness of the proposed control strategy against a sudden change in the solar radiation (e.g. passing cloud). For both scenarios the plant is represented by the nonlinear simulation model described by the system in (2) with a slight increase to thermal losses in order to make the scenarios more realistic. Field inlet temperature (T_{in}) and ambient temperature (T_a) are kept fixed at 189 °C and 28 °C respectively. Even though this may not be the case in the normal operation of the plant, this is still a reasonable assumption during the steady state phase. The HTF is assumed to be the synthetic oil Therminol® 55 and constrained to the range $0.002 - 0.012$ m^3/s where the minimum limit is normally for a safety reason. Exceeding a temperature of 305 °C puts the synthetic oil at the risk of being decomposed. The difference between the field outlet and inlet temperature is also constrained not to exceed 80 °C in order to avoid the risk of oil leakage Camacho et al. (2012). The latter has been taken care of implicitly when the nominal operating points and the desired reference temperature were selected. The HTF flow rate constraints are considered explicitly in the control design process as will be demonstrated in the following two scenarios.

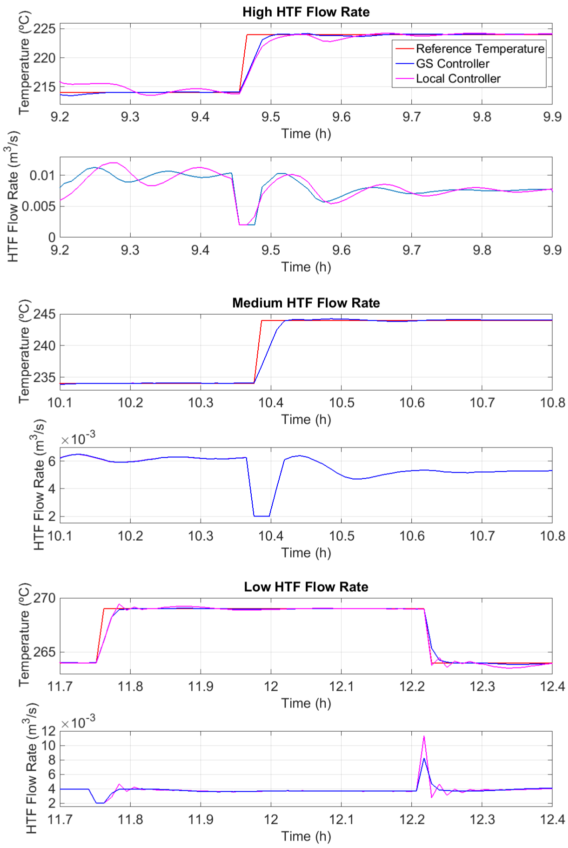

Fig. 3. First scenario: Control performance of a clear day.

5.1 *First Scenario– Clear Day*

Fig. 3 compares the control performance of the proposed GS control strategy with one of the local dual mode MPC controllers that was designed around the nominal operating point 0.006 m^3/s. For a clear day with a slowly time-varying solar radiation, the reference tracking and the associated control action around high, medium and low HTF flow rate are presented.

The GS controller shows excellent performance, coping with the slowly time-varying solar radiation over the whole range of operation with fast transients, with no overshoot and handling the flow rate constraints efficiently. Conversely, the local dual mode MPC controller performs well only in the region near the operating point where the corresponding linear model was identified (medium HTF flow rate). The oscillatory control performance of the local controller during high flow rates and the poor control performance during low flow rates with overshoot and severe control action can be seen clearly.

5.2 *Second Scenario– Cloudy Day*

The second scenario investigates the effect of a passing cloud on the GS control performance. Clouds act as a disturbance to the plant and therefore must be properly rejected. For a clear day with a slowly time-varying solar radiation around the mean of 674.75 W/m^2, the cloud is simulated by an extreme situation through a sudden drop in radiation with a relatively high level of noise. The scenario as illustrated in Fig. 4 starts with a typical plant

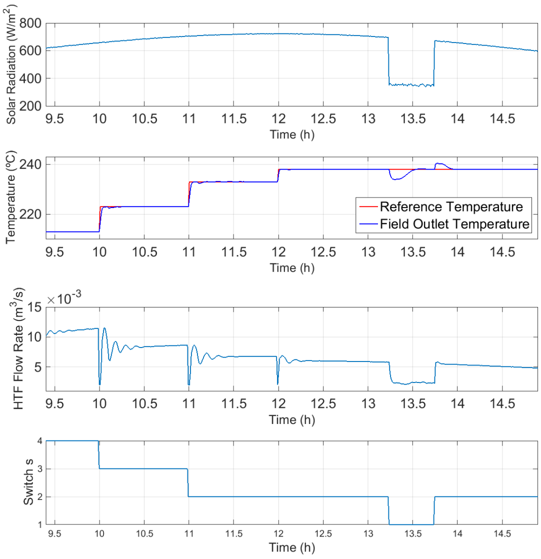

Fig. 4. Second scenario: Control performance of a cloudy day.

operation where a smooth switching between the local controllers in order to cope with the changing dynamics can be observed clearly. During the steady state operation of the plant around the nominal operating point 0.006 m^3/s a passing and persistent cloud passes by. The cloud drives the HTF to be decreased to around the operating condition 0.004 m^3/s where it gets handled by the corresponding controller sufficiently.

6. CONCLUSION

A GS dual mode MPC was developed in this paper to control the field outlet temperature of the ACUREX plant. The paper has continued the work started in Alsharkawi and Rossiter (2016) and extended some of the control strategies currently available in the literature. Specifically, compact LTI state space models around a family of operating points were estimated using a subspace identification method and corresponding dual mode MPC controllers within GS framework were designed. The estimated models have shown significant model order reduction when compared to the models available in the open literature while adequately capturing the phenomena of resonant modes. A fine decomposition of the plant region of operation has also been achieved through a best fit criterion as well as a systematic and online handling of the plant safety constraints over a wide range of operation. Feasibility and effectiveness of the proposed control strategy is demonstrated through two different and commonplace scenarios. The control strategy is shown to perform very well for both tracking and disturbance rejection and indeed superior to a single local controller.

As a final remark regarding the resonant modes of the plant, it should be pointed out that low order ARX models are not expected to capture these phenomena. This is evident from the poor control performance in Rato et al. (1997); Pickhardt (1998) when $3^{rd}-$order ARX models were estimated online in an adaptive control strategy. However, it can also be argued that the inappropriate selection of the scheduling variable is also contributing to the poor control performance as the actual flow rate of the HTF has not been taken into account.

One interesting question for future study is whether performance could be improved with an effective incorporation of feedforward term; this is an area which has received relatively little attention in the MPC literature.

REFERENCES

Alsharkawi, A. and Rossiter, J. (2016). Dual mode mpc for a concentrated solar thermal power plant. In *DYCOPS-CAB*.
Aringhoff, R., Association, E.S.T.P.I., Agreement, I.S.I., et al. (2005). *Concentrated Solar Thermal Power-Now!* Greenpeace.
Camacho, E.F., Berenguel, M., and Rubio, F.R. (1997). *Advanced control of solar plants*. Springer-Verlag.
Camacho, E.F., Berenguel, M., Rubio, F.R., and Martínez, D. (2012). *Control of solar energy systems*. Springer-Verlag.
Camacho, E., Rubio, F., Berenguel, M., and Valenzuela, L. (2007a). A survey on control schemes for distributed solar collector fields. part i: Modeling and basic control approaches. *Solar Energy*.
Camacho, E., Rubio, F., Berenguel, M., and Valenzuela, L. (2007b). A survey on control schemes for distributed solar collector fields. part ii: Advanced control approaches. *Solar Energy*.
Chisci, L., Falugi, P., and Zappa, G. (2003). Gain-scheduling mpc of nonlinear systems. *IJRNC*.
Goswami, D.Y., Kreith, F., and Kreider, J.F. (2000). *Principles of solar engineering*. CRC Press.
IEA (2014). *Key world energy statistics*. IEA.
Johansen, T.A., Hunt, K.J., and Petersen, I. (2000). Gain-scheduled control of a solar power plant. *CEP*.
Larimore, W.E. (1990). Canonical variate analysis in identification, filtering, and adaptive control. In *CDC*.
Leith, D.J. and Leithead, W.E. (2000). Survey of gain-scheduling analysis and design. *IJC*.
Ljung, L. (1995). *System identification toolbox: user's guide*. Citeseer.
Meaburn, A. and Hughes, F. (1993). Resonance characteristics of distributed solar collector fields. *Solar Energy*.
Philibert, C. (2010). *Technology roadmap: concentrating solar power*. OECD/IEA.
Pickhardt, R. (1998). Application of adaptive controllers to a solar power plant using a multi-model description. In *ACC*.
Rato, L., Borrelli, D., Mosca, E., Lemos, J., and Balsa, P. (1997). Musmar based switching control of a solar collector field. In *ECC*.
Rossiter, J.A. (2003). *Model-based predictive control: a practical approach*. CRC press.
Rugh, W.J. and Shamma, J.S. (2000). Research on gain scheduling. *Automatica*.
Stirrup, R., Loebis, D., Chipperfield, A., Tang, K., Kwong, S., and Man, K. (2001). Gain-scheduled control of a solar power plant using a hierarchical moga-tuned fuzzy pi-controller. In *ISIE*.
Van Overschee, P. and De Moor, B. (1996). *Subspace identification for linear systems: TheoryImplementationApplications*. Springer Science & Business Media.
Zhu, Y. (2001). *Multivariable system identification for process control*. Elsevier.